Partial 1420 MHz HI Survey of the North Polar Spur

Aaron Tran[1,3]
Isaac A. Domagalski[1,2], Caleb Levy[1,2]
Aaron Parsons[2,4,5], Garrett K. Keating[2,4,5], Baylee Bordwell[2,5]
[1]Central Intelligence Agency, 1000 Colonial Farm Rd, McLean, VA 22101, USA
[2]Dept. Astronomy, UC Berkeley, D-23 Hearst Field Annex, Berkeley, CA 94720, USA
[3]Dept. Earth and Planetary Science, UC Berkeley, 335 McCone Hall, Berkeley, CA 94720, USA
[4]Radio Astronomy Laboratory, UC Berkeley, Berkeley, CA 94720, USA
[5]Undergraduate Radio Laboratory teaching staff
Received in incomplete form 2014 May 6, revised 2014 May ?!

Abstract

We observe the north polar spur and stuff

1 Introduction

background on NPS. Supernovae, snowploughs, shocks, Sedov, whatever. ISM, physical properties inferable.

The North Polar Spur is a prominent ridge structure within the greater Loop-I region which emits continuum and HI line emission at 1420 MHz [*Heiles et al.*, 1980]

2 Observations

2.1 Leuschner radio dish

We use the Leuschner radio dish ($37°55'10.2''$ N, $-122°09'12.4''$ E), operated by UC Berkeley as part of Leuschner Observatory, to collect single-dish observations of the hyperfine HI line. The Leuschner radio dish, hereafter Leuschner (Figure 1), has diameter 3.6 m or 4.5 m depending on who is asked; the beamwidth is $\sim 4°$ at its operating frequency of 1420 MHz. Leuschner's view at low altitudes is blocked by surrounding hills; to the north Leuschner may point above $\sim 50°$, to the south Leuschner may point to 20–30° altitude. The Leuschner radio dish was originally built for the SETI Rapid Prototype Array near Leuschner Observatory, an early prototype for the now-underfunded and incomplete Allen Telescope Array. The dish has since been appropriated for undergraduate education; its sibling dishes have been dismantled or turned into gigantic bats (e.g., http://patriciavader.com/artwork/1696610_The_Giant_Bat.html).

RF waves incident on Leuschner are passed through a 200 MHz bandpass filter centered on 1420 MHz and mixed with a local oscillator (LO) signal of frequency $f_{\rm LO}$; both operations are performed at the antenna feed. The LO mixing sends frequencies of interest near 1420 MHz to intermediate frequencies ~ 150 MHz; this down-converted signal is routed to Leuschner Observatory facilities and bandpass filtered at 145–155 MHz.

We record an 8192 channel frequency spectrum with bandwidth 12 MHz centered on the intermediate frequency (IF) 150 MHz; spectral resolution is 1.5 kHz. Recall that IF frequencies correspond to radio frequencies $f - f_{\rm LO}$ (where f is radio sky frequency). The signal is digitized by an FPGA-based spectrometer using a polyphase filter bank; the effective sampling rate is 24 MHz. The signal of interest appears in our frequency output via Nyquist aliasing [*Siemion*, 2012].

For each point on the sky, we collect four raw spectra which are later reduced to a single calibrated spectrum. At a given LO frequency, we take two spectra: one with integration time 120 seconds, and one with integration time 12.5 seconds with a noise diode enabled. The noise diode injects power of a known temperature through the dish electronics, which permits us to convert spectrometer power to physical brightness temperature. We take two spectra for each of two LO frequencies $f_{\rm LO} = 1268.9$ MHz and $f_{\rm LO} = 1271.9$ MHz; this enables frequency-dependent gain correction. The intermediate frequency range 144–156 MHz thus corresponds to the radio frequency bands 1412.9–1424.9 MHz and 1415.9–1427.9 MHz respectively.

Figure 1. The Leuschner dish has beamwidth $\sim 4^\circ$ at 1420 MHz. Here the dish is shown with its erstwhile caretaker, *kartp* (courtesy of I. Domagalski, E. Herrera, K. Moses).

2.2 Observing campaign

Galactic coordinate definition, visible galaxy (RA, dec etc).

We observed the sky in the region $\{(l,b) \mid -150^\circ \leq l \leq 20^\circ, b \geq 0^\circ\}$, which contains the bulk of the North Polar Spur. Our observations were performed between 2014 April 26 to 2014 May 5. In order to completely map the sky, the region of interest should be sampled with angular spacing 2° (for beamwidth 4°); note that due to foreshortening, the spacing in galactic longitude is $2^\circ/\cos(b)$. Approximately 2500 pointings are required for complete sky coverage. Due to time constraints, we sampled most of the available region at 4° spacing in both galactic latitude/longitude.

Due to Leuschner's pointing limits, we are unable to collect data for a region roughly described by $\{(l,b) \mid -90^\circ \leq l \leq -20^\circ, 0^\circ \geq 38^\circ\}$. This blocks the base/stem of the spur, unfortunately, so we are limited to mapping the top and edges of the spur. From I. Domagalski's calculation, ~ 940 points of our mapping region are never visible; we imaged ~ 440 points and require ~ 1100 more points for complete coverage of the remainder of the visible sky.

Our observations zig-zag along lines of fixed longitude during each observing window (nighttime ~ 1600 to 0800 the next day), gradually incrementing in latitude from 0° to 90°. The status of ongoing observations may be monitored at http://ugastro.berkeley.edu/ domagalski/ay121/leuschner/status.html.

3 Data reduction

Our goal is to (1) convert unknown spectrometer intensity units to brightness temperature, and (2) remove the continuous bandpass filter

N.B. we may use the words power, intensity, and temperature interchangeably. Apologies for the technical imprecision... (I have not gone through and done the usual litany of checking that terms are defined at first usage and consistently used, not swapped out for synonyms)

I don't think I've presented/explained our spectra usage well (i.e. sticking to a certain convention when explaining spectra)

3.1 Radio frequency interference

The radio spectrum from 1400 to 1427 MHz is internationally allocated for Earth exploration, space research, and radio astronomy (as of May 5, 2014). However, we observe radio frequency interference (RFI) at 1420 MHz. A 2001 RFI survey with the Rapid Prototype Array (RPA) near Leuschner Observatory [*Harp and Ackerman*, 2001] found no satellite RFI frequency near 1420 MHz; only the sun contributed significant interference. However, out-of-band signals from aeronautical radionavigation (960–1215 MHz) and telecommunications (various bands between 1350–1525 MHz) may also interfere with our observations. Since 2001, we expect that interference from communication signals should have increased substantially.

RFI appears as sharp power spikes in output frequency spectra. The quantity of interference spikes is highly variable (Figure 2). We did not explore how RFI may vary with altitude and azimuth or time of day.

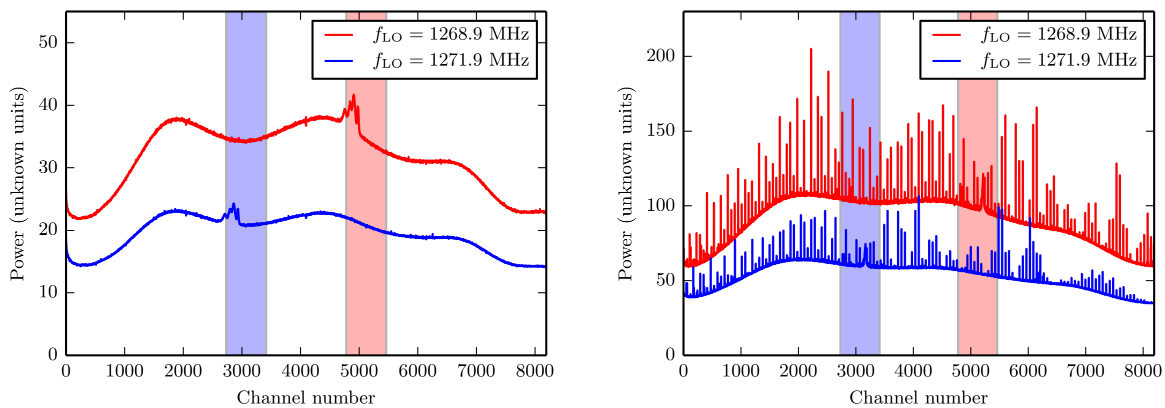

Figure 2. Raw spectra from each of two pointings show relatively low (left) and high (right) RFI. Channels correspond to different radio frequencies depending on f_{LO}, corresponding colored boxes for each LO frequency highlight the 1 MHz band centered on 1420.4 MHz. Note that spectra for different pointings have differing bandpass filter shapes and gains. Pointing coordinates are $l = 232.05°$, $b = 4°$ (left), $l = 16.01°$, $b = 20°$ (right). Raw spectra collected with noise diode for calibration are not shown but have comparable shapes, increased power offset, and increased noise.

We removed RFI spikes by binning spectra into bins of 4 channels and taking the bin channel with minimum power. We choose bin width 4 because our RFI spikes are typically localized to a single spectrometer channel, at most $2 - 3$ channels. Although ad hoc, this procedure empirically appears to work reasonably well.

3.2 Calibration

Prior to intensity calibration, we discard the 200 channels on each side of the spectra (without noise diode). The difference between spectra with and without noise should be proportional to noise diode temperature times frequency (channel) dependent gain. Figure 3 illustrates the effect of enabling noise diode.

To compare the system gain and temperature from multiple spectra, we need to remove the HI line. In all spectra we excise the region between 1419–1421.5 MHz (Figure 4) before processing.

For each set of spectra at a given f_{LO} we sum the channel-by-channel quotient between spectra with and without noise diode to estimate the gain effected by the noise diode. The noise diode adds $T \approx 100$ K and so we may calculate the gain

I wrote out the math for this procedure some time ago and it makes sense qualitatively, but Caleb's procedure is slightly different – it seems as if we compute the system temperature once for each set of spectra, and gain for left/right spectra.

Finally, in order to combine the left and right spectra, I averaged together BOTH the temperatures AND the frequencies of the data for the arrays corresponding the high and low Local Oscillator frequencies. As

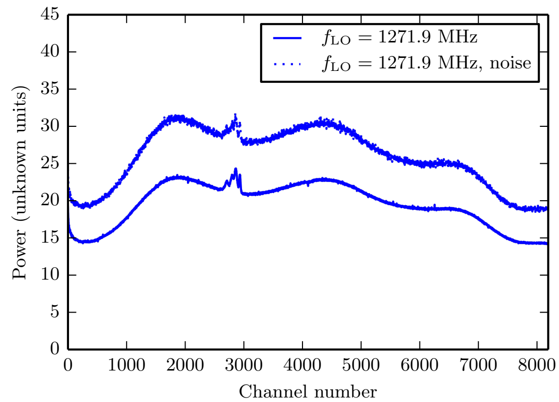

Figure 3. Spectra with (dots) and without (line) noise diode enabled. Same pointing as for left subplot of Figure 2.

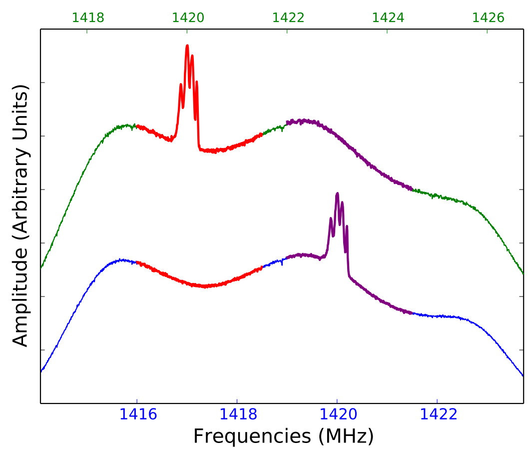

Figure 4. Excision procedure for system temperature and gain determination. Red, purple colors indicate region of the spectra that are removed in system temperature calculation. Same colors (i.e. spectral lines) are used to make a first pass at subtracting bandpass gain shape. Image is courtesy of C. Levy.

the indices for each frequency are different, I thought this was a good compromise; this does produce errors of order 10 khz however, so it is possible that this biases our data one way or another if the RF spikes have a systematic patter to them. It would probably be worth discussing this. – CALEB

3.3 Error analysis

Integration times were chosen so error would be nice (mainly for noise). Integration time for main observations dictated by physical brightness temp.

I chose the time for noise diode integration so that the error (which arises from a sum/average over all channels) would be order 10% of the channel-by-channel error.

The signal error is calculated as

5

Output frequency range is 1419 to 1421.5 MHz

4 Data analysis

4.1 Baseline removal and peak identification

Due to a shortage of time, I did not finish my own velocity computation etc... scripts. Mainly needed baseline fitting/removal, peak identification. (but, after baseline removal, I'd be able to get the main science done). Working on it now would require branching Isaac's pipeline, and risk messing up the current data processing pipeline. So I shan't do that yet...

Later on, I really want to be able to decompose the various peaks. It looks like our spur observations don't have multiple peaks anyways, so it's not so bad since we don't care about the galactic plane.

4.2 n-th moment computation

4.3 Data interpolation and projection

5 Results

5.1 Maps of the North Polar Spur

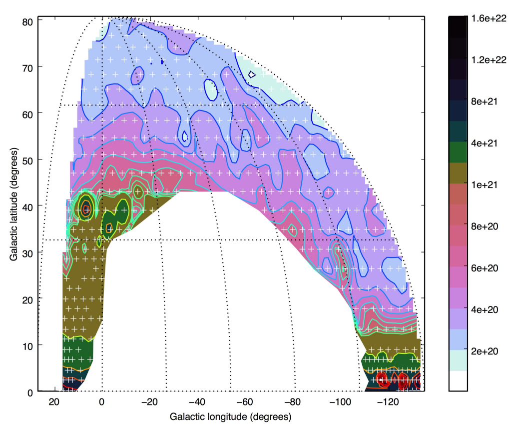

Figure 5. Column density. Note that this is very roughly log scaled.

Things to do:

- Manually compute Gaussian image interpolation
- Apply NaN mask to make imshow/contour/contourf plots better (instead of using a polygon to mask unmapped region). Maybe finish implementing signed distance function here to map out non-rectangular plot domain.
- Compare imshow/contour vs. contourf/contour. Imshow is continuous, technically carries more information.
- Consider conformal (stereographic), orthographic projections. Possibly include multiple images to replicate what a ground observer might see.
- Since we are not doing a complete sky map (which is what Mollweide is commonly used for), does there exist a more appropriate equal-area projection? Sinusoidal, Hammer, Aitoff, etc.

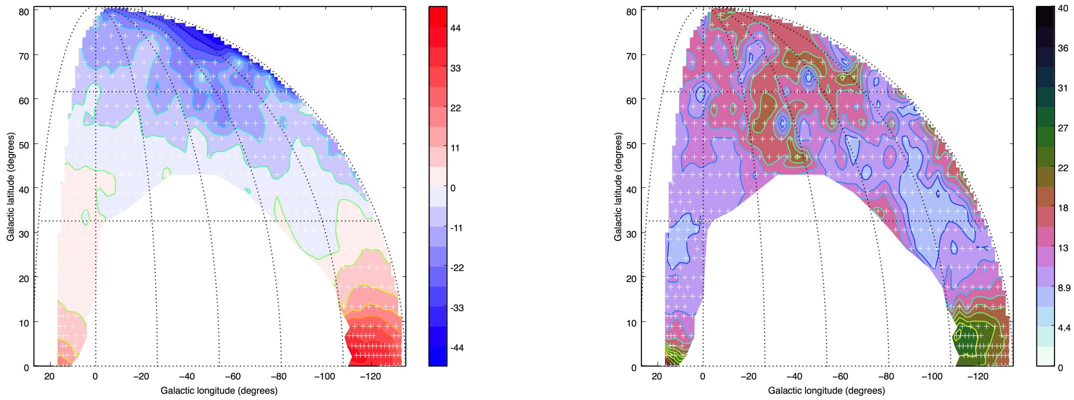

Figure 6. Mean velocity (left), stdev of velocity (right)

- Test colormaps in a systematic way. Determine physiologically sensible colormaps (i.e. no rainbows, jets)
- Determine best nonlinear colormapping for column density (logarithmic, power law). Maybe look at histogram and find the most "histogram-equalizing" transformation.
- Reduce the load times for both png and pdf... they're really slow. Maybe I should resort to jpg (welp, ugly, no)
- Multiple dimensions in color image – encode velocity (hue) and column density (brightness) together, with column density nonlinearly scaled.

5.2 Qualitative features

Comparing the dispersion to the velocity mean looks promising! As we might expect, dispersion is stronger towards the center of our postulated/expected bubble, a more robust velocity signal is seen at edges.

6 Discussion

6.1 Physical interpretation of observations

IF I separate out lines and get individual linewidths etc (by gaussian fit, dispersion for indiv peaks, however you like) – start considering physical phenomena that give rise to broadening.

Comparison, if there is time: download 1.4 GHz survey data from skyview.gsfc.nasa.gov and generate a comparison plot with same/similar projection.

6.2 Data reduction biases

RFI removal and calibration, and spectrum processing, naturally introduces biases. To remove RFI, we binned the frequency channels into groups of four and took the minimum value in each bin. Although this kills spikes, this also systematically biases our data downwards, particularly the channel readings where the HI line is present. We identify the selected bins with the ORIGINAL, ACTUAL frequency tied to that channel (so, the shape is roughly preserved, but the very peaks may be lost). We also introduce a more uneven frequency spacing and are throwing away data – this may increase error, although compared to the error of missing an RFI spike this may be a reasonable trade-off!

Caleb's procedure of throwing away 200 pts at edges of spectra – again, we are losing some (relatively unimportant) information. But, it helps cut down noise in the summation (more integration time, after a fashion).

6.3 RFI mitigation

Radio frequency interference was not actively characterized and addressed in this study. We suggest several approaches to addressing RFI in future work.

The quantity of interference signal is highly variable, with some spectra slathered in spikes and other spectra relatively unaffected. We speculate there may be multiple explanations. (1) geostationary satellites at fixed az-alt may contaminate certain pointings – this could be mitigated with prior knowledge of satellite az/alt. (2) airplanes. (3) if the RFI is from ground based transmission – e.g. if there are fewer transmissions at a certain time of day, or there is a directional dependence to broadcasts (wherever radio towers are located).

(if there is time – supply az,alt,time of pointings) (it would be nice to create a measure of how much RFI is present, then plot against az,alt to see if there is a portion of the sky that is particularly susceptible to contamination. We could do this with just our data for an incomplete, uneven survey, but it would be something.) (and, also plot the temporal dependance)

Tabulate list of sources https://casper.berkeley.edu/wiki/images/8/82/RPA5.pdf, see also VLA lists for examples.

Any future all-sky survey undertaken with the leuschner dish in May might want to map this region of the sky, then write the dish tracking script to avoid it. also keep track of where the sun and moon are.

If there is any way to probe polarization (as it seems they were once able to do with the RPA interferometer), we might be able to identify signals with strong polarization as being affiliated with human transmission [*Harp and Ackerman*, 2001].

7 Conclusions

Pretty pictures are gr8.

8 Appendix A: rainbow colormap considered harmful

Comparison plots for different colormaps.

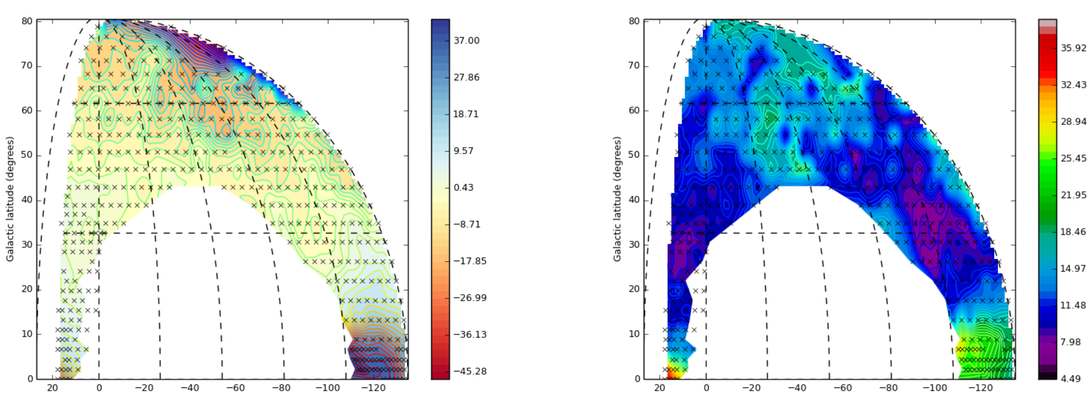

Figure 7. Mean velocity (left), stdev of velocity (right). Units are km/s for colors.

They look so pretty... but they're not as meaningful as they seem.

9 Acknowledgments

Figure 8. (image courtesy of I. Domagalski, E. Herrera, K. Moses)

Kartp noster, qui es in radiolab:
sanctificetur nomen tuum;
adveniat regnum tuum;
fiat voluntas tua.
sicut in academia, et in universitas.
Observationem nostrum cotidianum da nobis hodie;
et dimitte nobis errores nostra,
sicut et nos dimittimus erroribus nostris;
et ne nos inducas in tentationem;
sed libera nos a circumsonum.

Five pieces of duct tape.

10 Author contributions

I. A. D. did almost everything tracking. C. L. did all calibration. A. T. did some of the tracking. All parties contributed to debugging.

11 Electronic supplement

All supporting files are stored on the repository:
https://github.com/aarontran/ay121/lab4/.

12 References

Condon, J. J. and S. M. Ransom (2006), Essential Radio Astronomy, http://www.cv.nrao.edu/course/astr534/ERA.shtml.

Green, R. M. (1985), *Spherical astronomy*, 520pp., Cambridge Univ. Press, Cambridge.

Harp, G. R. and R. F. Ackermann (2001), RFI Survey at the RPA, https://casper.berkeley.edu/wiki/images/f/f9/RPA11.pdf.

Heiles, C., Y.-H. Chu, R. J. Reynolds, I. Yegingil, and T. H. Troland (1980), A new look at the North Polar Spur, *Astrophys. J.*, *242*, 533–540, doi:10.1086/158487.

Siemion, A. (2012), Leuschner Spectrometer, CASPER documentation wiki, https://casper.berkeley.edu/wiki/Leuschner_Spectrometer.

Wolleben, M. (2007), A New Model for the Loop I (North Polar Spur) Region, *Astrophys. J.*, *664*, 349–356, doi:10.1086/518711.